A Particle-Partition of Unity Method
Part VIII: Hierarchical Enrichment

Marc Alexander Schweitzer

no. 378

Diese Arbeit ist mit Unterstützung des von der Deutschen Forschungsgemeinschaft getragenen Sonderforschungsbereichs 611 an der Universität Bonn entstanden und als Manuskript vervielfältigt worden.

Bonn, Februar 2008

A Particle-Partition of Unity Method Part VIII: Hierarchical Enrichment

Marc Alexander Schweitzer

Institut für Numerische Simulation, Universität Bonn, Wegelerstr. 6, D-53115 Bonn, Germany
schweitzer@ins.uni-bonn.de

Summary. This paper is concerned with automatic enrichment in the particle-partition of unity method (PPUM). The goal of our automatic enrichment is to recover the optimal convergence rate of the uniform h-version independent of the regularity of the solution. Hence, we employ enrichment not only for modeling purposes but rather to improve the approximation properties of the numerical scheme. To this end we enrich our PPUM function space in an automatically determined enrichment zone hierarchically near the singularities of the solution. To overcome the ill-conditioning of the enriched shape functions we present an appropriate local preconditioner. The results of our numerical experiments clearly show that the hierarchically enriched PPUM recovers the optimal convergence rate globally and even shows a kind of superconvergence within the enrichment zone. The condition number of the stiffness matrix is independent of the employed enrichment and the relative size of the enrichment zone.

Key words: meshfree method, partition of unity method, extrinsic enrichment, preconditioning

1 Introduction

Singular and discontinuous enrichment functions are used for the modeling of e.g. cracks in many meshfree methods [5, 20], the extended finite element method (XFEM) [4, 6, 18], the generalized finite element method (GFEM) [10–12] or the particle-partition of unity method (PPUM) [22]. In most cases, the considered enrichment functions serve the purpose of modeling only. Hence the approximation properties of the resulting numerical scheme are limited by the regularity of the solution and no improvement in the asymptotic convergence rate is obtained. A naive approach to overcome this issue is the use of a predefined constant enrichment zone [21]. This however leads to a fast growth of the condition number of the stiffness matrix and thereby has an adverse effect on the overall accuracy of the approximation. In [7] the use of an additional cut-off function which controls the enrichment zone was suggested.

This approach yields some improvement, i.e. a less severe increase of the condition number. However, ultimately an ill-conditioned stiffness matrix arises also in this approach. The observed deterioration of the condition number can be remedied only by an appropriate basis transformation and projection—in essence a special preconditioner.

In this paper we focus on enrichment of the PPUM, however, the presented techniques can be applied also to other PU-based enrichment schemes. In particular we present an hierarchical enrichment procedure which defines an intermediate enrichment zone for the discretization. For each patch within this intermediate enrichment zone we construct a *local* basis transformation and a *local* projection (i.e. a special *local* preconditioner) which eliminates the *global* ill-conditioning due to the enrichment functions completely. The presented scheme attains a stable discretization independent of the employed enrichment functions and an optimal global convergence rate of the uniform h-version; i.e., the uniform h-version converges globally with a rate that is *not* limited by the regularity of the solution. For instance we obtain an $O(h)$ convergence in the energy-norm using linear polynomials globally. Within the enrichment zone the local convergence behavior is even $O(h^{1+\delta})$ with $\delta > 0$ in the energy-norm.

The remainder of this paper is organized as follows. In Section 2 we give a short review of the essential ingredients of the multilevel PPUM. In Section 3 we introduce our hierarchical enrichment scheme and the construction of our local preconditioner which yields a stable basis of the global PPUM space independent of the employed enrichment. The results of our numerical experiments are given in Section 4. These results clearly show that we obtain an optimal convergence behavior of the uniform h-version of the PPUM globally and that the condition number of the stiffness matrix does not suffer from the employed enrichment. Within the enrichment zone we obtain an almost quadratic convergence using linear polynomials only. Finally, we conclude with some remarks in Section 5.

2 Particle–Partition of Unity Method

In this section let us shortly review the core ingredients of the PPUM, see [14, 15, 21] for details. In a first step, we need to construct a PPUM space V^{PU}, i.e., we need to specify the PPUM shape functions $\varphi_i \vartheta_i^n$ where the functions φ_i form a partition of unity (PU) on the domain Ω and the functions ϑ_i^n denote the associated approximation functions considered on the patch $\omega_i := \mathrm{supp}(\varphi_i)$, i.e. polynomials ψ_i^s or enrichment functions η_i^t. With these shape functions, we then set up a sparse linear system of equations $A\tilde{u} = \hat{f}$ via the classical Galerkin method. The linear system is then solved by our multilevel iterative solver [15,17]. However, we need to employ a non-standard variational formulation of the PDE to account for the fact that our PPUM

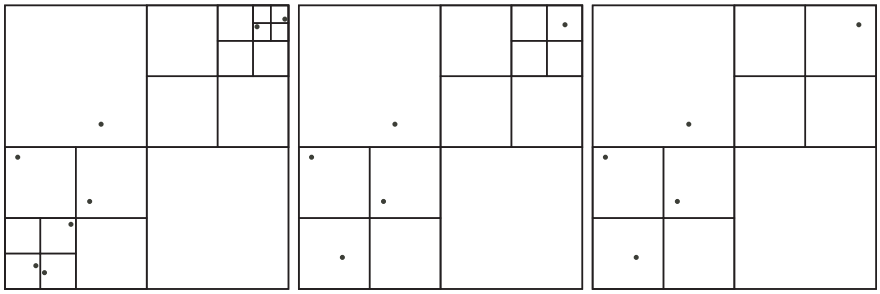

Fig. 1. Subdivision corresponding to a cover on level $J = 4$ with initial point cloud (left), derived coarser subdivisions on level 3 (center), and level 2 (right) with respective coarser point cloud.

shape functions—like most meshfree shape functions—do not satisfy essential boundary conditions explicitly.

The fundamental construction principle employed in [14] for the construction of the PU $\{\varphi_i\}$ is a d-binary tree. Based on the given point data $P = \{x_i \,|\, i = 1, \dots, \hat{N}\}$, we sub-divide a bounding-box $\mathcal{C}_\Omega \supset \Omega$ of the domain Ω until each cell

$$\mathcal{C}_i = \prod_{l=1}^{d} (c_i^l - h_i^l, c_i^l + h_i^l)$$

associated with a leaf of the tree contains at most a single point $x_i \in P$, see Figure 1. We obtain an overlapping cover $C_\Omega := \{\omega_i\}$ from this tree by defining the cover patches ω_i by

$$\omega_i := \prod_{l=1}^{d} (c_i^l - \alpha h_i^l, c_i^l + \alpha h_i^l), \quad \text{with } \alpha > 1. \tag{2.1}$$

Note that we define a cover patch ω_i for leaf-cells $\mathcal{C}_i$ that contain a point $x_i \in P$ as well as for *empty* cells that do not contain any point from P. The coarser covers C_Ω^k are defined considering coarser versions of the constructed tree, i.e., by removing a complete set of leaves of the tree, see Figure 1. For details of this construction see [14, 15, 21].

To obtain a PU on a cover C_Ω^k with $N_k := \operatorname{card}(C_\Omega^k)$ we define a weight function $W_{i,k} : \Omega \to \mathbb{R}$ with $\operatorname{supp}(W_{i,k}) = \omega_{i,k}$ for each cover patch $\omega_{i,k}$ by

$$W_{i,k}(x) = \begin{cases} \mathcal{W} \circ T_{i,k}(x) & x \in \omega_{i,k} \\ 0 & \text{else} \end{cases} \tag{2.2}$$

with the affine transforms $T_{i,k} : \overline{\omega}_{i,k} \to [-1, 1]^d$ and $\mathcal{W} : [-1, 1]^d \to \mathbb{R}$ the reference d-linear B-spline. By simple averaging of these weight functions we obtain the functions

$$\varphi_{i,k}(x) := \frac{W_{i,k}(x)}{S_{i,k}(x)}, \quad \text{with} \quad S_{i,k}(x) := \sum_{l=1}^{N_k} W_{l,k}(x). \tag{2.3}$$

We refer to the collection $\{\varphi_{i,k}\}$ with $i = 1, \ldots, N_k$ as a partition of unity since there hold the relations

$$\begin{aligned} 0 \;\leq\; \varphi_{i,k}(x) \leq 1, \qquad & \sum_{i=1}^{N_k} \varphi_{i,k} \equiv 1 \text{ on } \overline{\Omega}, \\ \|\varphi_{i,k}\|_{L^\infty(\mathbb{R}^d)} \leq C_{\infty,k}, \qquad & \|\nabla\varphi_{i,k}\|_{L^\infty(\mathbb{R}^d)} \leq \frac{C_{\nabla,k}}{\operatorname{diam}(\omega_{i,k})} \end{aligned} \tag{2.4}$$

with constants $0 < C_{\infty,k} < 1$ and $C_{\nabla,k} > 0$ so that the assumptions on the PU for the error analysis given in [2] are satisfied by our PPUM construction. Furthermore, the PU (2.3) based on the cover C_Ω^k obtained from the scaling of a tree decomposition with $\alpha > 1$ satisfies

$$\mu(\{x \in \omega_{i,k} \,|\, \varphi_{i,k}(x) = 1\}) \approx \mu(\omega_{i,k}),$$

i.e., the PU has the flat-top property, see [17,22]. This ensures that the product functions $\varphi_{i,k}\vartheta_{i,k}^n$ are linearly independent, provided that the employed local approximation functions $\vartheta_{i,k}^n$ are linearly independent with respect to $\{x \in \omega_{i,k} \,|\, \varphi_{i,k}(x) = 1\}$. Hence, we obtain global stability of the product functions $\varphi_{i,k}\vartheta_{i,k}^n$ from the local stability of the approximation functions $\vartheta_{i,k}^n$.

In general the local approximation space $V_{i,k} := \operatorname{span}\langle\vartheta_{i,k}^n\rangle$ associated with a particular patch $\omega_{i,k}$ of a PPUM space V_k^{PU} consists of two parts: A smooth approximation space, e.g. polynomials $\mathcal{P}^{p_{i,k}}(\omega_{i,k}) := \operatorname{span}\langle\psi_i^s\rangle$, and an enrichment part $\mathcal{E}_{i,k}(\omega_{i,k}) := \operatorname{span}\langle\eta_i^t\rangle$, i.e.

$$V_{i,k}(\omega_{i,k}) = \mathcal{P}^{p_{i,k}}(\omega_{i,k}) + \mathcal{E}_{i,k}(\omega_{i,k}) = \operatorname{span}\langle\psi_i^s, \eta_i^t\rangle.$$

Note that for the smooth space $\mathcal{P}^{p_{i,k}}$ we employ a local basis $\psi_{i,k}^s$ on $\omega_{i,k}$, i.e. $\psi_{i,k}^s = p_s \circ T_{i,k}$ and $\{p_s\}$ denotes a stable basis on $[-1,1]^d$. The enrichment functions $\eta_{i,k}^t$ however are often given as global functions η^t on the computational domain Ω since they are designed to capture special behavior of the solution at a particular location. Therefore, the restrictions $\eta_{i,k}^t := \eta^t|_{\omega_{i,k}}$ of the enrichment functions η^t to a particular patch $\omega_{i,k}$ may be ill-conditioned or even linearly dependent on $\omega_{i,k}$, even if the enrichment functions η^t are well-conditioned on a global scale. Furthermore, the coupling between the spaces $\mathcal{P}^{p_{i,k}}$ and $\mathcal{E}_{i,k}$ on the patch $\omega_{i,k}$ must be considered. The set of functions $\{\psi_{i,k}^s, \eta_{i,k}^t\}$ will also degenerate from a basis of $V_{i,k}$ to a generating system only, if the restricted enrichment functions $\eta_{i,k}^t = \eta^t|_{\omega_{i,k}}$ can be well approximated by polynomials $\psi_{i,k}^s$ on the patch $\omega_{i,k}$.

Remark 1. The elimination of these linear dependencies and the selection of an appropriate basis $\langle\tilde{\vartheta}_{i,k}^m\rangle$ for the space $V_{i,k}(\omega_{i,k})$ is the main challenge in an enriched PPUM computation (and any other numerical method that employs enrichment). To this end we have developed a projection operator or preconditioner

$$\Pi_{i,k}^* : \operatorname{span}\langle\vartheta_{i,k}^n\rangle \to \operatorname{span}\langle\tilde{\vartheta}_{i,k}^m\rangle$$

that maps the ill-conditioned generating system $\langle \psi_{i,k}^s, \eta_{i,k}^t \rangle = \langle \vartheta_{i,k}^n \rangle$ to a stable basis $\langle \tilde{\vartheta}_{i,k}^m \rangle$, see Section 3.

With the help of the shape functions $\varphi_{i,k}\vartheta_{i,k}^n$ we then discretize a PDE in weak form

$$a(u,v) = \langle f, v \rangle$$

via the classical Galerkin method to obtain a discrete linear system of equations $A\tilde{u} = \hat{f}$. Note that the PU functions (2.3) in the PPUM are in general piecewise rational functions only. Therefore, the use of an appropriate numerical integration scheme is indispensable in the PPUM as in most meshfree approaches [1, 3, 8, 9, 15]. Moreover, the functions $\varphi_{i,k}\vartheta_{i,k}^n$ in general do not satisfy the Kronecker property. Thus, the coefficients $\tilde{u}_k := (u_{i,k}^n)$ of a discrete function

$$u_k^{\mathrm{PU}} = \sum_{i=1}^{N_k} \varphi_{i,k} \sum_{n=1}^{d_{i,k}} u_{i,k}^n \vartheta_{i,k}^n = \sum_{i=1}^{N_k} \varphi_{i,k} \Big(\sum_{s=1}^{d_{i,k}^{\mathcal{P}}} u_{i,k}^s \psi_{i,k}^s + \sum_{t=1}^{d_{i,k}^{\mathcal{E}}} u_{i,k}^{t+d_{i,k}^{\mathcal{P}}} \eta_{i,k}^t \Big) \tag{2.5}$$

with $d_{i,k}^{\mathcal{P}} := \dim \mathcal{P}_{i,k}$, $d_{i,k}^{\mathcal{E}} := \dim \mathcal{E}_{i,k}$ and $d_{i,k} := d_{i,k}^{\mathcal{P}} + d_{i,k}^{\mathcal{E}}$ on level k do not directly correspond to function values and a trivial interpolation of essential boundary data is not available.

2.1 Essential Boundary Conditions

The treatment of essential boundary conditions in meshfree methods is not straightforward and a number of different approaches have been suggested. In [16] we have presented how Nitsche's method [19] can be applied successfully in the meshfree context. Here, we give a short summary of this approach. To this end, let us consider the model problem

$$\begin{aligned} -\mathbf{div}\,\boldsymbol{\sigma}(u) &= f && \text{in } \Omega \subset \mathbb{R}^d \\ \boldsymbol{\sigma}(u) \cdot n &= g_N && \text{on } \Gamma_N \subset \partial\Omega \\ u \cdot n &= g_{D,n} && \text{on } \Gamma_D = \partial\Omega \setminus \Gamma_N \\ (\boldsymbol{\sigma}(u) \cdot n) \cdot t &= 0 && \text{on } \Gamma_D = \partial\Omega \setminus \Gamma_N \end{aligned} \tag{2.6}$$

In the following we drop the level subscript $k = 0, \ldots, J$ for the ease of notation.

Let us define the cover of the Dirichlet boundary

$$C_{\Gamma_D} := \{\omega_i \in C_\Omega \,|\, \Gamma_{D,i} \neq \emptyset\}$$

where $\Gamma_{D,i} := \omega_i \cap \Gamma_D$ and $\gamma_{D,i} := \mathrm{diam}(\Gamma_{D,i})$. With these conventions we define the cover-dependent functional

$$J_{C_\Omega}(w) := \int_\Omega \boldsymbol{\sigma}(w) : \boldsymbol{\epsilon}(w)\, dx - 2\int_{\Gamma_D} (n \cdot \boldsymbol{\sigma}(w) n) n \cdot w\, ds + \beta \sum_{\omega_i \in C_{\Gamma_D}} \gamma_{D,i}^{-1} \int_{\Gamma_{D,i}} (w \cdot n)^2\, ds$$

with some parameter $\beta > 0$. Minimizing J_{C_Ω} with respect to the error $u - u^{\mathrm{PU}}$ yields the weak formulation

$$a_{C_\Omega}(w, v) = l_{C_\Omega}(v) \quad \text{for all } v \in V^{\mathrm{PU}} \tag{2.7}$$

with the cover-dependent bilinear form

$$\begin{aligned} a_{C_\Omega}(u, v) := &\int_\Omega \boldsymbol{\sigma}(u) : \boldsymbol{\epsilon}(v)\ dx - \int_{\Gamma_D} (n \cdot \boldsymbol{\sigma}(u)n)n \cdot v\ ds \\ &- \int_{\Gamma_D} (n \cdot \boldsymbol{\sigma}(v)n)n \cdot u\ ds + \beta \sum_{\omega_i \in C_{\Gamma_D}} \gamma_{D,i}^{-1} \int_{\Gamma_{D,i}} u \cdot nv \cdot n\ ds \end{aligned}$$

and the corresponding linear form

$$\langle l_{C_\Omega}, v\rangle := \int_\Omega fv + \int_{\Gamma_N} g_N v - \int_{\Gamma_D} g_{D,n}(n \cdot \boldsymbol{\sigma}(v)n) + \beta \sum_{\omega_i \in C_{\Gamma_D}} \gamma_{D,i}^{-1} \int_{\Gamma_{D,i}} g_{D,n} v \cdot n\ ds$$

There is a unique solution u^{PU} of (2.7) if the regularization parameter β is chosen large enough; i.e., the regularization parameter $\beta = \beta_{V^{\mathrm{PU}}}$ is dependent on the discretization space V^{PU}. This solution u^{PU} satisfies optimal error bounds if the space V^{PU} admits the inverse estimate

$$\|(n \cdot \boldsymbol{\sigma}(v)n)\|^2_{-\frac{1}{2}, C_{\Gamma_D}} \ \leq\ C^2_{V^{\mathrm{PU}}} \|v\|^2_E \ =\ C^2_{V^{\mathrm{PU}}} \int_\Omega \boldsymbol{\sigma}(v) : \boldsymbol{\epsilon}(v)\ dx \tag{2.8}$$

for all $v \in V^{\mathrm{PU}}$ with respect to the cover-dependent norm

$$\|w\|^2_{-\frac{1}{2}, C_{\Gamma_D}} := \sum_{\omega_i \in C_{\Gamma_D}} \gamma_{D,i} \|w\|^2_{L^2(\Gamma_{D,i})}$$

with a constant $C_{V^{\mathrm{PU}}}$ depending on the cover C_Ω and the employed local bases $\langle \vartheta_i^n \rangle$ only. If $C_{V^{\mathrm{PU}}}$ is known, the regularization parameter $\beta_{V^{\mathrm{PU}}}$ can be chosen as $\beta_{V^{\mathrm{PU}}} > 2C^2_{V^{\mathrm{PU}}}$ to obtain a symmetric positive definite linear system [19]. Hence, the main task associated with the use of Nitsche's approach in the PPUM context is the efficient and automatic computation of the constant $C_{V^{\mathrm{PU}}}$, see [16, 21]. To this end, we consider the inverse assumption (2.8) as a generalized eigenvalue problem locally on each patch $\omega_i \in C_{\Gamma_D}$ and solve for the largest eigenvalue to obtain an approximation of $C^2_{V^{\mathrm{PU}}}$.

In summary, the PPUM discretization of our model problem (2.6) using the space V^{PU} on the cover C_Ω is carried out in two steps: First, we estimate the regularization parameter $\beta_{V^{\mathrm{PU}}}$ from (2.8). Then, we define the weak form (2.7) and use Galerkin's method to set up the respective symmetric positive definite linear system $A\tilde{u} = \hat{f}$. This linear system is then solved by our multilevel iterative solver [15, 17].

3 Hierarchical Enrichment and Local Preconditioning

The use of smooth polynomial local approximation spaces $V_{i,k} = \mathcal{P}^{p_{i,k}}$ in our PPUM is optimal only for the approximation of a smooth or regular solution u. In the case of a discontinuous and singular solution u there are essentially two approaches we can pursue: First, a classical adaptive refinement process which essentially resolves the singular behavior of the solution by geometric subdivision, see [17,22]. Second, an algebraic approach that is very natural to the PPUM, the explicit enrichment of the global approximation space by special shape functions η^s. This approach is also pursued in other meshfree methods [5, 20], the XFEM [4, 6, 18] or the GFEM [10–12]. Most enrichment schemes however focus on modeling issues and not on approximation properties or the conditioning of the resulting stiffness matrix.

In this section we introduce an automatic hierarchical enrichment scheme for our PPUM that provides optimal convergence properties and avoids an ill-conditioning of the resulting stiffness matrix due to enrichment. To this end, we consider a reference problem from linear elastic fracture mechanics

$$\begin{aligned} -\mathbf{div}\,\boldsymbol{\sigma}(u) &= f \quad \text{in } \Omega = (-1,1)^2, \\ \boldsymbol{\sigma}(u)\cdot n &= g_N \text{ on } \Gamma_N \subset \partial\Omega \cup C, \\ u &= g_D \text{ on } \Gamma_D = \partial\Omega \setminus \Gamma_N. \end{aligned} \tag{3.1}$$

The internal traction-free segment

$$C := \{(x,y) \in \Omega \,|\, x \in (-0.5, 0.5) \text{ and } y = 0\}$$

is referred to as a crack. The crack C induces a discontinuous displacement field u across the crack line C with singularities at the crack tips $c_l := (-0.5, 0)$ and $c_u := (0.5, 0)$. Hence, the local approximation spaces $V_{i,k}$ employed in our PPUM must respect these features to provide good approximation.

The commonly used enrichment strategy employs simple geometric information only. A patch $\omega_{i,k}$ (or an element) is enriched by the discontinuous Haar function if the patch is (completely) cut by the crack C, i.e.

$$\mathcal{E}_{i,k} := H^C_{\pm}\mathcal{P}^{p_{i,k}} \quad \text{and} \quad V_{i,k} := \mathcal{P}^{p_{i,k}} + H^C_{\pm}\mathcal{P}^{p_{i,k}}. \tag{3.2}$$

Note that in fact most other enrichment procedures employ $\mathcal{E}_{i,k} = H^C_{\pm}$ only. If the patch $\omega_{i,k}$ contains a crack tip ξ_{tip}, i.e. $c_l \in \omega_{i,k}$ or $c_u \in \omega_{i,k}$, then the patch is enriched by the respective space of singular tip functions

$$W_{\text{tip}} := \{\sqrt{r}\cos\frac{\theta}{2}, \sqrt{r}\sin\frac{\theta}{2}, \sqrt{r}\sin\theta\sin\frac{\theta}{2}, \sqrt{r}\sin\theta\cos\frac{\theta}{2}\} \tag{3.3}$$

given in local polar coordinates with respect to the tip ξ_{tip}, i.e. $\mathcal{E}_{i,k} = W_{\text{tip}}|_{\omega_{i,k}}$. This yields the local approximation space

$$V_{i,k} := \mathcal{P}^{p_{i,k}} + W_{\text{tip}}$$

for a patch $\omega_{i,k}$ that contains the tip ξ_{tip}. Let us summarize this geometric modeling enrichment scheme in the following classifier function $e^M : C_\Omega^k \to \{\texttt{lower\_tip}, \texttt{upper\_tip}, \texttt{jump}, \texttt{none}\}$

$$e^M(\omega_{i,k}) := \begin{cases} \texttt{lower\_tip} & \text{if } c_l \in \omega_{i,k} \text{ and } c_u \notin \omega_{i,k}, \\ \texttt{upper\_tip} & \text{if } c_l \notin \omega_{i,k} \text{ and } c_u \in \omega_{i,k}, \\ \texttt{jump} & \text{if } \{c_l, c_u\} \cap \omega_{i,k} = \emptyset \text{ and } C \cap \omega_{i,k} \neq \emptyset, \\ \texttt{none} & \text{else.} \end{cases} \tag{3.4}$$

Note that the direct evaluation of e^M for all patches $\omega_{i,k} \in C_\Omega^k$ requires $O(N_k)$ rather expensive geometric operations such as line-line intersections.

Even though this enrichment is sufficient to model a crack and captures the asymptotic behavior of the solution at the tip, this strategy suffers from various drawbacks. With respect to the discontinuous enrichment the main issue is that very small intersections of a patch with a crack cause an ill-conditioned stiffness matrix which can compromise the stability of the discretization; e.g. when the volumes of the sub-patches induced by the cut with the crack differ substantially in size. This is usually circumvented by a predefined geometric tolerance parameter which rejects such small intersections. In the case of a one-dimensional enrichment space $\mathcal{E}_{i,k} = H_\pm^C$ this approach is sufficient—if the tolerance parameter is chosen relative to the diameter of the patch. For a multi-dimensional enrichment space $\mathcal{E}_{i,k} = H_\pm^C \mathcal{P}^{p_{i,k}}$ this approach can be too restrictive to obtain optimal results.

The crack tip enrichment space W_{tip} given in (3.3) models the essential behavior of the solution at the tip. However, the singularity at the tip has a substantially larger zone of influence than just the containing patch. Therefore, the simple geometric modeling enrichment (3.4) is not sufficient to improve the asymptotic convergence behavior of the employed numerical scheme.

These issues can be overcome with the help of our multilevel sequence of covers C_Ω^k and a local preconditioner. Starting on the coarsest level $k = 0$ of our cover sequence we consider the cover $C_\Omega^0 = \{\omega_{i,0}\}$ and define the intermediate enrichment classifier $I_0 : C_\Omega^0 \to \{\texttt{lower\_tip}, \texttt{upper\_tip}, \texttt{jump}, \texttt{none}\}$ by the geometric/modeling enrichment scheme discussed above

$$I_0(\omega_{i,0}) := e^M(\omega_{i,0}).$$

In the next step we define the associated intermediate enrichment spaces $\mathcal{E}_{i,k}^I$ for $k = 0$

$$\mathcal{E}_{i,k}^I := \begin{cases} W_{c_l} & \text{if } \texttt{lower\_tip} = I_k(\omega_{i,k}), \\ W_{c_u} & \text{if } \texttt{upper\_tip} = I_k(\omega_{i,k}), \\ H_\pm^C \mathcal{P}^{p_{i,k}} & \text{if } \texttt{jump} = I_k(\omega_{i,k}) \text{ and } C \cap \omega_{i,k} \neq \emptyset, \\ 0 & \text{else.} \end{cases} \tag{3.5}$$

with $d_{i,k}^{\mathcal{E}^I} := \text{card}(\{\eta_{i,k}^t\})$ and the respective intermediate approximation spaces

$$V_{i,k}^I := \mathcal{P}^{p_{i,k}} + \mathcal{E}_{i,k}^I = \operatorname{span}\langle \psi_{i,k}^s, \eta_{i,k}^t \rangle = \operatorname{span}\langle \vartheta_{i,k}^n \rangle$$

with $d_{i,k}^{V^I} := d_{i,k}^{\mathcal{P}} + d_{i,k}^{\mathcal{E}^I}$ and $d_{i,k}^{\mathcal{P}} = \dim(\mathcal{P}^{p_{i,k}})$. Using all functions $\vartheta_{i,k}^n$, i.e. $\psi_{i,k}^s$ and $\eta_{i,k}^t$, we setup the local mass matrix $M_{i,k}$ with the entries

$$(M_{i,k})_{m,n} := \int_{\omega_{i,k} \cap \Omega} \vartheta_{i,k}^n \vartheta_{i,k}^m \, dx \quad \text{for all } m,n = 1, \dots, d_{i,k}^{\mathcal{V}^{\mathcal{I}}}. \tag{3.6}$$

From the eigenvalue decomposition

$$O_{i,k}^T M_{i,k} O_{i,k} = D_{i,k} \quad \text{with } O_{i,k}, D_{i,k} \in \mathbb{R}^{d_{i,k}^{V^I} \times d_{i,k}^{V^I}} \tag{3.7}$$

of the matrix $M_{i,k}$ where

$$O_{i,k}^T O_{i,k} = \mathbb{I}_{d_{i,k}^{V^I}}, \qquad (D_{i,k})_{m,n} = 0 \quad \text{for all } m \neq n$$

we can extract a stable basis $\langle \tilde{\vartheta}_{i,k}^m \rangle$ by a simple cut-off of small eigenvalues. To this end let us assume that the eigenvalues $(D_{i,k})_{m,m}$ are given in decreasing order, i.e. $(D_{i,k})_{m,m} \geq (D_{i,k})_{m+1,m+1}$. Then we can easily partition the matrices $O_{i,k}^T$ and $D_{i,k}$ as

$$O_{i,k}^T = \begin{pmatrix} \tilde{O}_{i,k}^T \\ K_{i,k}^T \end{pmatrix}, \quad D_{i,k} = \begin{pmatrix} \tilde{D}_{i,k} & 0 \\ 0 & \kappa_{i,k} \end{pmatrix}$$

where the mth row of the rectangular matrix $\tilde{O}_{i,k}^T$ is an eigenvector of $M_{i,k}$ that is associated with an eigenvalue $(D_{i,k})_{m,m} = (\tilde{D}_{i,k})_{m,m} \geq \epsilon \, (D_{i,k})_{0,0}$ and $K_{i,k}^T$ involves all eigenvectors that are associated with small eigenvalues. Since $(\tilde{D}_{i,k})_{m,m} \geq \epsilon \, (D_{i,k})_{0,0}$ the operator

$$\mathit{\Pi}_{i,k}^* := \tilde{D}_{i,k}^{-1/2} \tilde{O}_{i,k}^T$$

is well-defined and can be evaluated stably. Furthermore, the projection $\mathit{\Pi}_{i,k}^*$ removes the near-null space of $M_{i,k}$ due to the cut-off parameter ϵ and we have

$$\mathit{\Pi}_{i,k}^* M_{i,k} (\mathit{\Pi}_{i,k}^*)^T = \tilde{D}_{i,k}^{-1/2} \tilde{O}_{i,k}^T M_{i,k} O_{i,k} \tilde{D}_{i,k}^{-1/2} = \mathbb{I}_{d_{i,k}^{\mathit{\Pi}}}$$

where $d_{i,k}^{\mathit{\Pi}} := \operatorname{card}\{(D_{i,k})_{m,m} \geq \epsilon \, (D_{i,k})_{0,0}\}$ denotes the row-dimension of $\tilde{O}_{i,k}^T$ and $\mathit{\Pi}_{i,k}^*$. Hence, the operator $\mathit{\Pi}_{i,k}^*$ maps the ill-conditioned generating system $\langle \vartheta_{i,k}^n \rangle = \langle \psi_{i,k}^s, \eta_{i,k}^t \rangle$ to a basis $\langle \tilde{\vartheta}_{i,k}^m \rangle$ that is optimally conditioned — it is an optimal preconditioner.

Assuming that the employed local basis $\langle \psi_{i,k}^s \rangle$ is well-conditioned and that ϵ is small we have $\mathcal{P}^{p_{i,k}} \subset \operatorname{span}\langle \tilde{\vartheta}_{i,k}^m \rangle$ so that if $\dim(\mathcal{P}^{p_{i,k}}) = d_{i,k}^{\mathit{\Pi}}$ we can remove the enrichment functions $\eta_{i,k}^t$ completely from the local approximation space and use $V_{i,k} = \mathcal{P}^{p_{i,k}}$. Therefore, we define our final enrichment indicator $E_k : C_\Omega^k \to \{\texttt{lower\_tip}, \texttt{upper\_tip}, \texttt{jump}, \texttt{none}\}$ on level k as

$$E_k(\omega_{i,k}) := \begin{cases} I_k(\omega_{i,k}) \text{ if } \dim(\mathcal{P}^{p_{i,k}}) \neq d_{i,k}^{\Pi}, \\ \texttt{none} \quad \text{else.} \end{cases} \tag{3.8}$$

The local approximation space $V_{i,k}$ assigned to an enriched patch $\omega_{i,k}$ is given by

$$V_{i,k} := \Pi_{i,k}^* V_{i,k}^I = \text{span}\langle \tilde{\vartheta}_{i,k}^m \rangle \tag{3.9}$$

On the next finer level $k+1$ we utilize the geometric hierarchy of our cover patches to define our intermediate enrichment indicator I_{k+1}. Recall that for each cover patch $\omega_{i,k+1}$ there exists exactly one cover patch $\omega_{\tilde{i},k}$ such that $\omega_{i,k+1} \subset \omega_{\tilde{i},k}$, compare Figure 1. Hence we can define our intermediate enrichment indicator I_{k+1} on level $k+1$ as

$$I_{k+1}(\omega_{i,k+1}) := \begin{cases} E_k(\omega_{\tilde{i},k}) \text{ if } E_k(\omega_{\tilde{i},k}) \neq \texttt{jump}, \\ \texttt{jump} \quad \text{if } E_k(\omega_{\tilde{i},k}) = \texttt{jump} \text{ and } C \cap \omega_{i,k} \neq \emptyset, \\ \texttt{none} \quad \text{else} \end{cases}$$

directly from the enrichment indicator E_k on level k and a minimal number of geometric operations. With this intermediate enrichment indicator we apply the above scheme recursively to derive the enrichment indicators E_l for all levels $l = 1, \ldots, J$. Finally, we obtain stable local basis systems $\langle \tilde{\vartheta}_{i,l}^m \rangle$ and the respective approximation spaces $V_{i,l} = \text{span}\langle \tilde{\vartheta}_{i,l}^m \rangle$ for all cover patches $\omega_{i,l} \in C_\Omega^l$ on all levels $l = 0, \ldots, J$. Recalling that our PU functions $\varphi_{i,l}$ satisfy the flat-top condition (see Section 2) this is sufficient to obtain the stability of the global basis $\langle \varphi_{i,l} \tilde{\vartheta}_{i,l}^m \rangle$ for the PPUM space V_l^{PU} on level l.[1]

Remark 1. Note that we do not need to apply the local preconditioner $\Pi_{i,k}^*$ for the evaluation of the basis $\langle \varphi_{i,k} \tilde{\vartheta}_{i,k}^m \rangle$ in each quadrature point during the assembly of the stiffness matrix. It is sufficient to transform the stiffness matrix A_k^{GS} on level k which was assembled using the generating system $\langle \psi_{i,k}^s, \eta_{i,k}^t \rangle$ by the block-diagonal operator Π_k^* with the block-entries

$$(\Pi_k^*)_{g,h} := \begin{cases} \Pi_{g,k}^*, \, g = h \\ 0 \quad \text{else,} \end{cases}$$

for all $g = 1, \ldots, N_k$; i.e., we obtain the stiffness matrix A_k with respect to the basis $\langle \varphi_{i,k} \tilde{\vartheta}_{i,k}^m \rangle$ on level k as the product operator

$$A_k = \Pi_k^* A_k^{\text{GS}} (\Pi_k^*)^T.$$

Remark 2. Note that in the discussion above we have considered the identity operator $\mathbb{I}$ on the local patch $\omega_{i,k}$, i.e. the mass matrix $M_{i,k}$. However, we can construct the respective preconditioner also for different operators e.g. the

[1] Actually we need to apply the construction of the preconditioner to the operator $M_{i,k}^{\text{FT}}$ which involves integrals on $\{x \in \omega_{i,k} \,|\, \varphi_{i,k}(x) = 1\}$ instead of the complete patch $\omega_{i,k}$.

operator $-\Delta + \mathbb{I}$ which corresponds to the H^1-norm. In exact arithmetic and with a cut-off parameter $\epsilon = 0$ changing the operator in the above construction has an impact on the constants only. However, due to our cut-off parameter ϵ we may obtain a different subspace $\text{span}\langle\tilde{\vartheta}^m_{i,k}\rangle$ for different operators with the same ϵ.

3.1 Error Bound

Due to our hierarchical enrichment we obtain a sequence of PPUM spaces V_k^{PU} with $k = 0, \ldots, J$ that contain all polynomials up to degree $p_k = \min_i p_{i,k}$ on a particular level k and all enrichment functions η^t (up to the cut-off parameter ϵ) in the enrichment zone E on all levels k. Hence the global convergence rate of our enriched PPUM is not limited by the regularity of the solution u. To confirm this assertion let us consider the splitting

$$u = u_p + \tilde{\chi}_E u_s$$

where u_p denotes the regular part of the solution u, u_s the singular part, and $\tilde{\chi}_E$ is a mollified characteristic function of the enrichment zone E which contains all singular points of u, i.e. of u_s. Multiplication with $1 \equiv \sum_{i=1}^N \varphi_i$ yields

$$u = \sum_{i=1}^N \varphi_i u_p + \sum_{i=1}^N \varphi_i \tilde{\chi}_E u_s.$$

Let us further consider the PPUM function (we drop the level index k for the ease of notation in the following)

$$u^{\text{PU}} := \sum_{E(\omega_i)=\texttt{none}} \varphi_i \varpi_i + \sum_{E(\omega_i)\neq\texttt{none}} \varphi_i(\varpi_i + e_i)$$

where $E(\omega_i)$ denotes the enrichment indicator given in (3.8), $\varpi_i \in \mathcal{P}^{p_i}$ and $e_i \in \mathcal{E}_i$. For the ease of notation let us assume that $E(\omega_i) = \texttt{none}$ holds for all patches ω_i with $i = 1, \ldots, M-1$ and $E(\omega_i) \neq \texttt{none}$ holds for all patches ω_i with $i = M, \ldots, N$ so that we can write

$$u^{\text{PU}} = \sum_{i=1}^{M-1} \varphi_i \varpi_i + \sum_{i=M}^N \varphi_i(\varpi_i + e_i).$$

With the assumption

$$\text{supp}(\tilde{\chi}_E) \cap \bigcup_{i=1}^{M-1} \omega_i = \emptyset, \qquad \text{i.e.} \quad \tilde{\chi}_E \sum_{i=1}^{M-1} \varphi_i \equiv 0,$$

we can write the analytic solution u as

$$u = \sum_{i=1}^{M-1} \varphi_i u_p + \sum_{i=M}^{N} \varphi_i (u_p + \tilde{\chi}_E u_s)$$

and obtain the error with respect to the PPUM function u^{PU} as

$$u^{\mathrm{PU}} - u = \sum_{i=1}^{M-1} \varphi_i (\varpi_i - u_p) + \sum_{i=M}^{N} \varphi_i ((\varpi_i + e_i) - (u_p + \tilde{\chi}_E u_s)). \tag{3.10}$$

By the triangle inequality we have

$$\begin{aligned} \|u - u^{\mathrm{PU}}\| \leq \| \sum_{i=1}^{M-1} \varphi_i (\varpi_i - u_p)\| \\ + \| \sum_{i=M}^{N} \varphi_i ((\varpi_i + e_i) - (u_p + \tilde{\chi}_E u_s))\|. \end{aligned} \tag{3.11}$$

The first term on the right-hand side corresponds to the error of a PPUM approximation of a regular function with polynomial local approximation spaces. For the ease of notation let us assume $h = \mathrm{diam}(\omega_i)$ and $p_i = 1$ for all $i = 1, \ldots, N$, then we can bound this error term with the help of the standard PUM error analysis [2] by $O(h)$ in the H^1-norm, i.e.

$$\| \sum_{i=1}^{M-1} \varphi_i (\varpi_i - u_p)\|_{H^1} \leq O(h).$$

To obtain an upper bound for the second term of (3.11)

$$J_E := \| \sum_{i=M}^{N} \varphi_i ((\varpi_i + e_i) - (u_p + \tilde{\chi}_E u_s))\|$$

we consider the equality

$$u_p + \tilde{\chi}_E u_s = u_p + (\tilde{\chi}_E - 1)u_s + u_s$$

and attain an upper bound of J_E again by the triangle inequality

$$\begin{aligned} J_E &= \| \sum_{i=M}^{N} \varphi_i ((\varpi_i + e_i) - (u_p + (\tilde{\chi}_E - 1)u_s + u_s))\| \\ &\leq \| \sum_{i=M}^{N} \varphi_i (\varpi_i - (u_p + (\tilde{\chi}_E - 1)u_s))\| \\ &\quad + \| \sum_{i=M}^{N} \varphi_i (e_i - u_s)\|. \end{aligned}$$

The function $u_p + (\tilde{\chi}_E - 1)u_s$ is regular since $\tilde{\chi}_E = 1$ in the vicinity of the singular points of u_s. Hence, we can bound the first term on the right-hand side

$$\| \sum_{i=M}^{N} \varphi_i(\varpi_i - (u_p + (\tilde{\chi}_E - 1)u_s))\|_{H^1} \leq O(h)$$

again by $O(h)$. Assuming that the enrichment functions resolve the singular part u_s of the solution u we can choose $e_i = u_s$ and so the second term vanishes and we obtain the upper bound

$$\| \sum_{i=M}^{N} \varphi_i((\varpi_i + e_i) - \tilde{\chi}_E(u_p + u_s))\|_{H^1} \leq O(h)$$

for the error in $\text{supp}(\tilde{\chi}_E) \subset E$. This yields the error bound

$$\|u - u^{\text{PU}}\|_{H_1} \leq O(h)$$

for the global error on the domain Ω.

Note however that we can obtain a better estimate for the error in the enrichment zone; i.e., the hierarchically enriched PPUM shows a kind of superconvergence within the enrichment zone. To this end consider the case $u_s = 0$, i.e., the approximation of a regular solution $u = u_p$ by an enriched PPUM. Then, J_E becomes

$$J_E = \| \sum_{i=M}^{N} \varphi_i((\varpi_i + e_i) - u_p))\|$$

and the standard error bound $O(h)$ ignores all degrees of freedom collected in e_i which are associated with the restrictions $\eta^t|_{\omega_{i,k}}$ of the enrichment functions to the local patches. Globally, the functions η^t represent a specific (type of) singularity. The restrictions $\eta^t|_{\omega_{i,k}}$ however are regular functions (if the patch does not contain the singular points of η^t) and can improve the local approximation substantially. Hence, a better bound for J_E for regular solutions u can be attained.

For a singular solution $u_s \neq 0$ we can utilize this observation by considering the splitting of the enrichment part e_i on a particular patch in two local components $e_i = e_i^s + e_i^p$. On each patch ω_i with $i = M, \ldots, N$ this splitting can be chosen to balance the two error terms on the right-hand side of the inequality

$$\begin{aligned} J_E &= \| \sum_{i=M}^{N} \varphi_i((\varpi_i + e_i^p + e_i^s) - (u_p + \tilde{\chi}_E u_s))\| \\ &\leq \| \sum_{i=M}^{N} \varphi_i((\varpi_i + e_i^p) - (u_p + (\tilde{\chi}_E - 1)u_s))\| \\ &\quad + \| \sum_{i=M}^{N} \varphi_i(e_i^s - u_s)\|. \end{aligned}$$

This can yield a much smaller error since the regular function $u_p + (\tilde{\chi}_E - 1)u_s$ is now approximated by more degrees of freedom, i.e., by all polynomials and

a number of enrichment functions restricted to the local patch ω_i. Hence, the Galerkin solution which minimizes J_E (i.e. minimizes (3.10) with respect to the energy-norm) can show a much better convergence of $O(h^{1+\delta})$ with $\delta > 0$ in the enrichment zone than the global $O(h)$ behavior.

The impact of this observation is that the coefficients of the asymptotic expansion of the solution, e.g. the stress intensity factors, can be extracted from the solution with much higher accuracy and better convergence behavior in the enrichment zone than the global error bound implies.

Remark 3. Note that due to our cut-off parameter $\epsilon > 0$ our local function spaces $V_{i,k}$ may not contain all enrichment functions $\eta^t_{i,k}$. Especially we may encounter the situation that a particular patch $\omega_{i,k+1}$ employs less enrichment functions than its parent patch $\omega_{\tilde{i},k} \supset \omega_{i,k+1}$; i.e., the local approximation spaces $V_{i,k+1}$ and $V_{\tilde{i},k}$ are *nonnested* due to the cut-off. Hence, the parameter δ in the discussion given above may not be constant on all levels and the measured convergence rates can jump due to the cut-off.

4 Numerical Results

In this section we present some results of our numerical experiments using the hierarchically enriched PPUM discussed above. To this end, we introduce some shorthand notation for various norms of the error $u - u^{\mathrm{PU}}$, i.e., we define

$$e_{L^\infty} := \frac{\|u - u^{\mathrm{PU}}\|_{L^\infty}}{\|u\|_{L^\infty}}, e_{L^2} := \frac{\|u - u^{\mathrm{PU}}\|_{L^2}}{\|u\|_{L^2}}, e_{H^1} := \frac{\|u - u^{\mathrm{PU}}\|_{H^1}}{\|u\|_{H^1}}. \tag{4.1}$$

For each of these error norms we compute the respective algebraic convergence rate ρ by considering the error norms of two consecutive levels $l-1$ and l

$$\rho := -\frac{\log\left(\frac{\|u-u_l^{\mathrm{PU}}\|}{\|u-u_{l-1}^{\mathrm{PU}}\|}\right)}{\log(\frac{\mathsf{dof}_l}{\mathsf{dof}_{l-1}})}, \quad \text{where } \mathsf{dof}_k := \sum_{i=1}^{N_k} \dim(V_{i,k}). \tag{4.2}$$

Hence the optimal rate ρ_{H^1} of an uniformly h-refined sequence of spaces with $p_{i,k} = p$ for all $i = 1, \ldots, N_k$ and $k = 0, \ldots, J$ for a regular solution u is $\rho_{H^1} = \frac{p}{d}$ where d denotes the spatial dimension of $\Omega \subset \mathbb{R}^d$. This corresponds to the classical $h^{\gamma_{H^1}}$ notation with $\gamma_{H^1} = \rho_{H^1} d = p$.

To assess the quality of our hierarchical enrichment scheme we consider the simple model problem

$$\begin{aligned} -\Delta u &= f \ \text{ in } \Omega = (-1,1)^2 \subset \mathbb{R}^2, \\ u &= g \ \text{ on } \partial\Omega, \end{aligned} \tag{4.3}$$

where we choose f and g such that the analytic solution u is given by

$$u(x,y) = \sqrt{r}(\sin\frac{\theta}{2} + \cos\frac{\theta}{2})(1+\sin\theta) + (x^2-1) + (y^2-1) + 1 \tag{4.4}$$

Table 1. Relative errors e (4.1) and convergence rates ρ (4.2) with respect to the complete domain Ω.

J	dof	N	e_{L^∞}	ρ_{L^∞}	e_{L^2}	ρ_{L^2}	e_{H^1}	ρ_{H^1}
1	28	4	7.262_{-2}	–	5.011_{-2}	–	1.663_{-1}	–
2	70	16	4.741_{-2}	0.47	3.096_{-2}	0.53	1.449_{-1}	0.15
3	226	64	1.614_{-2}	0.92	1.098_{-2}	0.88	8.826_{-2}	0.42
4	868	256	5.192_{-3}	0.84	2.974_{-3}	0.97	4.544_{-2}	0.49
5	3400	1024	1.488_{-3}	0.92	7.779_{-4}	0.98	2.296_{-2}	0.50
6	13456	4096	4.491_{-4}	0.87	1.990_{-4}	0.99	1.148_{-2}	0.50
7	53214	16384	1.317_{-4}	0.89	5.034_{-5}	1.00	5.864_{-3}	0.49
8	210036	65536	3.748_{-5}	0.92	1.266_{-5}	1.01	3.010_{-3}	0.49
9	837176	262144	1.042_{-5}	0.93	3.173_{-6}	1.00	1.405_{-3}	0.55
10	3288341	1048576	2.942_{-6}	0.92	8.078_{-7}	1.00	7.367_{-4}	0.47

where $r = r(x, y)$ and $\theta = \theta(x, y)$ denote polar coordinates, see Figure 2. This solution is discontinuous along the line

$$C := \{(x, y) \in \Omega \,|\, x \in (-1, 0) \text{ and } y = 0\}$$

and weakly singular at the point $(0, 0)$. The model problem (4.3) with the considered data f and g is essentially a scalar analogue of a linear elastic fracture mechanics problem such as (3.1). Hence, we employ the enrichment functions (3.2) and (3.3) with respect to the crack C in our computations.

We consider a sequence of uniformly refined covers C^k_Ω with $\alpha = 1.3$ in (2.1) and local polynomial spaces $\mathcal{P}^{p_{i,k}} = \mathcal{P}^1$ on all levels $k = 1, \ldots, J$ for the discretization of (4.3). The number of patches on level k is given by $N_k = 2^{2k}$. On the levels $k \leq 3$ we use the geometric/modeling indicator e^M (3.4) as enrichment indicator, on the finer levels $k > 3$ we use the recursively defined hierarchical enrichment indicator (3.8), see Section 3. Hence, the subdomain

$$E_{\text{tip}} := (-0.25, 0.25)^2 \subset \Omega = (-1, 1)^2 \tag{4.5}$$

denotes the initial enrichment zone with respect to the point singularity of (4.4) at $(0, 0)$ on the levels $k > 3$, see Figure 4.5. The respective intermediate local enrichment spaces $\mathcal{E}^I_{i,k}$ are defined by (3.5) and the resulting local approximation spaces $V_{i,k}$ by (3.9). The local preconditioner $\Pi^*_{i,k}$ is based on the local mass matrix and employs a cut-off parameter $\epsilon = 10^{-12}$.

Since the solution is singular at $(0, 0)$ a classical uniform h-version without enrichment (or just modeling enrichment) yields convergence rates (4.2) of $\rho_{L^2} = \frac{2}{3}$ and $\rho_{H^1} = \frac{1}{3}$ only. Due to our hierarchical enrichment we anticipate to recover the optimal convergence rates $\rho_{L^2} = 1$ and $\rho_{H^1} = \frac{1}{2}$ globally. The convergence behavior inside E_{tip} can be better, see Section 3.1.

We assess the quality of our local preconditioner $\Pi^*_{i,k}$ by studying the convergence behavior of our multilevel solver [13,15,21] applied to the enriched PPUM discretization using the transformed basis $\tilde{\vartheta}^m_{i,k}$ locally. We denote the respective linear system on level k by

$$A_k \tilde{u}_k = \hat{f}_k, \tag{4.6}$$

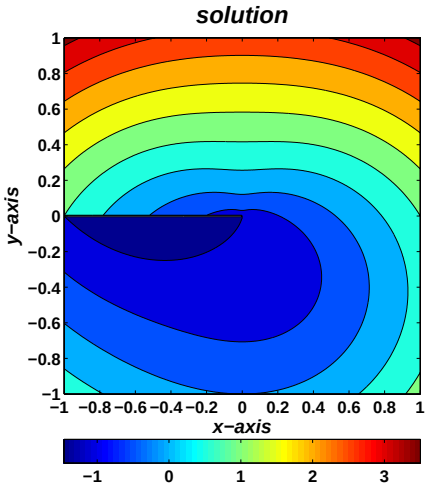

Fig. 2. Contour plot of the solution (4.4).

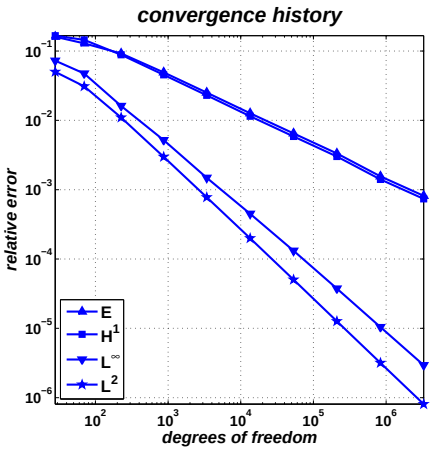

Fig. 3. Convergence history of the measured relative errors e (4.1) with respect to the complete domain Ω in the L^∞-norm, the L^2-norm, the H^1-norm, and the energy-norm on the respective level (denoted by E in the legend).

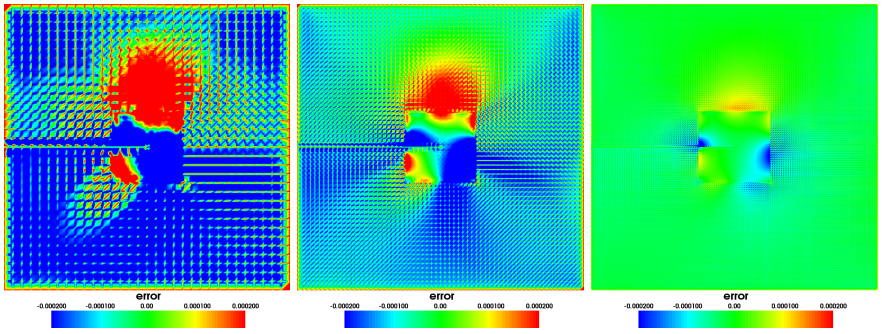

Fig. 4. Contour plot of the error $u_k^{\mathrm{PU}} - u$ for $k = 5, 6, 7$ (from left to right).

where $\tilde{u}_k := (u_{i,k}^m)$ denotes the coefficient vector associated with the PPUM function

$$u_k^{\mathrm{PU}} = \sum_{i=1}^{N_k} \varphi_{i,k} \sum_{m=1}^{d_{i,k}} u_{i,k}^m \tilde{\vartheta}_{i,k}^m$$

and $\hat{f}$ denotes a moment vector with respect to the PPUM basis functions $\langle \varphi_{i,k}\ \tilde{\vartheta}_{i,k}^m \rangle$ on level k.

We employ a standard $V(1,1)$-cycle with block-Gauß–Seidel smoother [13, 15, 21] for the iterative solution of (4.6). We consider three choices for

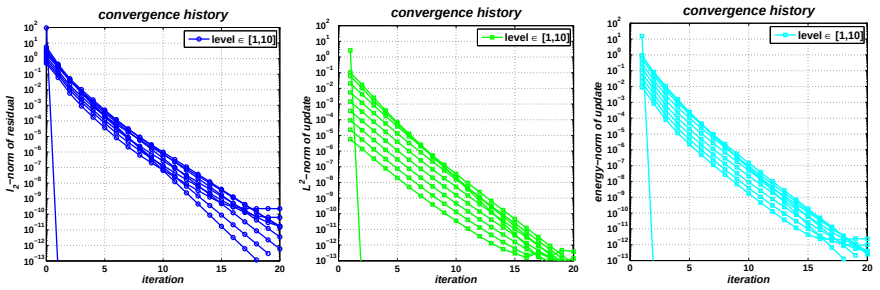

Fig. 5. Convergence history for a $V(1,1)$-cycle multilevel iteration with block-Gauß–Seidel smoother and nested iteration initial guess (left: convergence of residual vector (4.8) in the l^2-norm, center: convergence of iteration update (4.7) in the L^2-norm, right: convergence of iteration update (4.7) in the energy-norm).

the initial guess: First, a nested iteration approach, where the solution u_k^{PU} obtained on level k is used as initial guess on level $k+1$. Note that this approach avoids unphysical oscillations in the initial guess which can otherwise spoil the convergence of the iterative solution process. Therefore, we also consider the choices of a vanishing initial guess and a random valued initial guess for the iterative solver to enforce these unphysical oscillations in the initial guess. The condition number of the iteration matrix is bounded by a constant if the asymptotic convergence rate of the iterative solver is independent of the number of levels. In our context this also means that we find no deterioration of the condition number due to the enrichment.

In Figure 3 we give the plots of the relative errors with respect to the L^∞-norm, the L^2-norm, the H^1-norm, and the energy-norm. From these plots and the respective convergence rates ρ_{L^∞}, ρ_{L^2}, and ρ_{H^1} given in Table 1 we can clearly observe the anticipated optimal global convergence of our hierarchically enriched PPUM with $\rho_{L^2} = 1$ and $\rho_{H^1} = \frac{1}{2}$. On level $k = 10$ we obtain 7 digits of relative accuracy in the L^2-norm and 4 digits in the H^1-norm. In Figure 4 we have depicted contour plots of the error $u_k^{\mathrm{PU}} - u$ for levels $k = 5, 6, 7$ using the same scaling for all plots. We can clearly see the enrichment zone E_{tip} from these plots and observe the fast reduction of the error due to the refinement.

The convergence behavior of our multilevel solver with a nested iteration initial value is depicted in Figure 5. We consider the convergence of the iterative update $c_{k,\mathrm{iter}}^{\mathrm{PU}}$ associated with the coefficient vector

$$\tilde{c}_{k,\mathrm{iter}} := \tilde{u}_{k,\mathrm{iter}} - \tilde{u}_{k,\mathrm{iter}-1} \tag{4.7}$$

with respect to the L^2-norm and the energy-norm as well as the convergence of the residual vector

$$\hat{r}_{\mathrm{iter}} := \hat{f}_k - A_k \tilde{u}_{k,\mathrm{iter}} \tag{4.8}$$

in the l^2-norm. All depicted lines are essentially parallel with a gradient of -0.25 indicating that the convergence rate of our multilevel solver is 0.25 and

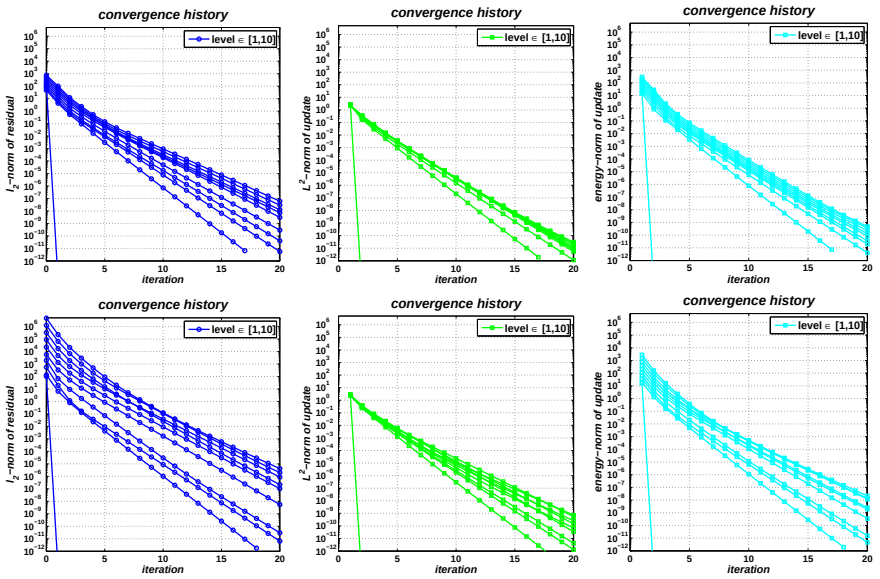

Fig. 6. Convergence history for a $V(1,1)$-cycle multilevel iteration with block-Gauß–Seidel smoother and zero (upper row) and random (lower row) initial guess (left: convergence of residual vector (4.8) in the l^2-norm, center: convergence of iteration update (4.7) in the L^2-norm, right: convergence of iteration update (4.7) in the energy-norm).

independent of the number of levels and thereby independent of the number of enriched patches and the number of enrichment functions. In Figure 6 we give the respective convergence behavior using a vanishing initial guess and a random valued initial guess to enforce the presence of unphysical oscillations in the (early) iterates. Again we observe that all depicted lines have essentially the same gradient -0.25 which is identical to the lines given in Figure 5. Hence, there is no amplification of unphysical oscillations and our multilevel solver converges with the same rate of 0.25 independent of the employed initial value. The convergence behavior of our iterative multilevel solver is independent of the number of patches and the number of enrichment degrees of freedom. Therefore, the condition number of the iteration matrix is stable and independent of these parameters. Our hierarchical enrichment scheme with local preconditioning avoids a deterioration of the condition number and thereby a deterioration of the stability due to the enrichment completely.

Finally, let us focus on the local convergence properties of our enriched PPUM discretization within the enrichment zone E_{tip} (4.5). To this end, we define three subdomains

$$E_1 := E_{\text{tip}} = \Big(-\frac{1}{4}, \frac{1}{4}\Big)^2, \quad E_2 := \Big(-\frac{1}{8}, \frac{1}{8}\Big)^2, \quad E_2 := \Big(-\frac{1}{16}, \frac{1}{16}\Big)^2 \tag{4.9}$$

Table 2. Relative errors e (4.1) and convergence rates ρ (4.2) with respect to the subsets E_1, E_2, and E_3 from (4.9).

J	dof	N	e_{L^∞}	ρ_{L^∞}	e_{L^2}	ρ_{L^2}	e_{H^1}	ρ_{H^1}
with respect to E_1								
2	28	4	4.329_{-2}	0.94	3.245_{-2}	1.03	9.040_{-2}	0.72
3	70	16	3.145_{-2}	0.35	2.061_{-2}	0.50	6.313_{-2}	0.39
4	178	36	1.058_{-2}	1.17	5.325_{-3}	1.45	2.559_{-2}	0.97
5	562	100	3.385_{-3}	0.99	1.390_{-3}	1.17	9.671_{-3}	0.85
6	2002	324	1.018_{-3}	0.95	3.534_{-4}	1.08	3.495_{-3}	0.80
7	7248	1156	2.965_{-4}	0.96	8.867_{-5}	1.07	1.272_{-3}	0.79
8	25926	4356	8.477_{-5}	0.98	2.217_{-5}	1.09	4.629_{-4}	0.79
9	100298	16900	2.387_{-5}	0.94	5.539_{-6}	1.03	1.577_{-4}	0.80
10	340007	66564	6.648_{-6}	1.05	1.745_{-6}	0.95	3.933_{-4}	−0.75
with respect to E_2								
3	28	4	1.659_{-2}	1.23	1.178_{-2}	1.33	3.599_{-2}	1.00
4	112	16	4.200_{-3}	0.99	3.707_{-3}	0.83	1.216_{-2}	0.78
5	252	36	1.209_{-3}	1.54	8.846_{-4}	1.77	4.271_{-3}	1.29
6	700	100	3.040_{-4}	1.35	2.133_{-4}	1.39	1.472_{-3}	1.04
7	2268	324	7.329_{-5}	1.21	5.210_{-5}	1.20	5.182_{-4}	0.89
8	7500	1156	1.819_{-5}	1.17	1.287_{-5}	1.17	1.901_{-4}	0.84
9	26576	4356	4.555_{-6}	1.09	3.202_{-6}	1.10	7.596_{-5}	0.72
10	101194	16900	1.671_{-6}	0.75	1.072_{-6}	0.82	6.574_{-5}	0.11
with respect to E_3								
4	28	4	3.567_{-3}	1.69	2.447_{-3}	1.80	1.096_{-2}	1.35
5	112	16	9.241_{-4}	0.97	7.710_{-4}	0.83	4.124_{-3}	0.70
6	252	36	2.651_{-4}	1.54	1.803_{-4}	1.79	1.471_{-3}	1.27
7	700	100	6.244_{-5}	1.42	4.338_{-5}	1.39	5.247_{-4}	1.01
8	2268	324	1.495_{-5}	1.22	1.056_{-5}	1.20	1.882_{-4}	0.87
9	7376	1156	3.685_{-6}	1.19	2.612_{-6}	1.18	8.269_{-5}	0.70
10	26470	4356	1.794_{-6}	0.56	9.266_{-7}	0.81	6.490_{-5}	0.19

and measure the relative errors (4.1) and convergence rates (4.2) with respect to E_1, E_2, and E_3 of (4.9). According to Section 3.1 we anticipate to find a faster convergence within the enrichment zone $_{\text{tip}}$ than for the complete domain Ω. The plots given in Figure 7 and the measured rates displayed in Table 2 clearly show this anticipated behavior. Note that we find about 6 digits of relative accuracy in the L^2-norm and about 4 digits in the H^1-norm on E_1, i.e. in the vicinity of the singularity. Up to level $k = 9$ we find $\rho_{H^1} \approx 0.8$ within the subdomains E_1, E_2, and E_3 whereas globally we have the optimal rate $\rho_{H^1} = 0.5$. Hence, we obtain a convergence behavior better than $O(h^{3/2})$ in the enrichment zone with respect to the energy-norm using enriched linear local approximation spaces only.

On level $k = 10$ however we find a sharp jump in the measured convergence rates. For the H^1-norm we even find an increase in the error on level $k = 10$ compared with level $k = 9$. Recall from Remark 3 that we may not expect the measured convergence rates to be constant due to the employed cut-off in the construction of our projection $\Pi^*_{i,k}$ which can yield nonnested local approximation spaces. The projection operators $\Pi^*_{i,k}$ employed in this computation were based on the identity operator, i.e. on the L^2-norm. Hence, we have eliminated enrichment functions whose contribution to the approximation of the L^2-norm is insubstantial. This however may not be true for the H^1-norm.

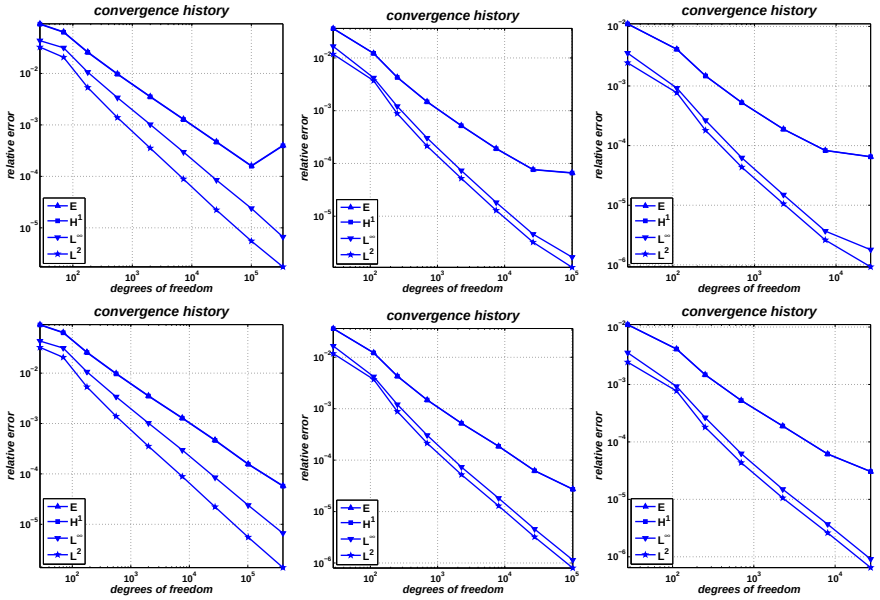

Fig. 7. Convergence history of the measured relative errors e (4.1) with respect to the subdomains E_1 (left), E_2 (center), and E_3 (right) given in (4.9) with respect to the L^∞-norm, the L^2-norm, the H^1-norm, and the energy-norm on the respective level (denoted by E in the legend). The upper row refers to the enriched PPUM using a preconditioner based on the L^2-norm, i.e., the local mass matrix, the lower row refers to the enriched PPUM using a preconditioner based on the H^1-norm, i.e., the local stiffness matrix.

According to Remark 2 changing the operator in the construction of $\Pi^*_{i,k}$ can impact the cut-off behavior. Constructing the projection $\Pi^*_{i,k}$ based on the operator $-\Delta + \mathbb{I}$ yields an elimination of functions that contribute insubstantially to the H^1-norm. This can eliminate (or will at least reduce) the jumps of the measured convergence rates for the H^1-norm (and weaker norms). From the numbers given in Table 3 where we employ a projection $\Pi^*_{i.k}$ based on the H^1-norm we can clearly observe this anticipated improvement, see also Figure 7. Now we have $\rho_{H^1} > 0.5$ on all levels and $\rho_{H^1} \approx 0.7$ on level $k = 10$ for E_1. In Figure 8 we have depicted the enrichment patterns within E_{tip} for the projections based on the L^2-norm and on the H^1-norm. For each patch $\omega_{i,k} \subset E_{\text{tip}}$ on level $k = 9, 10$ we have plotted the dimension of the local approximation space $V_{i,k}$, i.e., the number of shape functions $\tilde{\vartheta}^m_{i,k}$ after cut-off. From these plots we can clearly observe that more enrichment functions are present in the H^1-based approach on level $k = 10$ than for the L^2-based projection. On level $k = 9$ the enrichment patterns are almost identical and so are the measured errors, compare Table 2 and Table 3. On level $k = 10$ however we see a substantial reduction in degrees of freedom due to the cut-

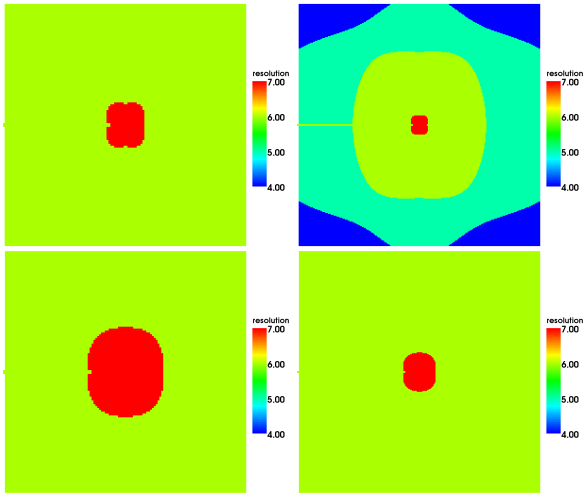

Fig. 8. Enrichment pattern on levels $k = 9$ (left) and $k = 10$ (right) within the enrichment zone E_{tip}. Color coded is the dimension of the local approximation space $\dim(V_{i,k}) = \text{card}(\{\tilde{\vartheta}^m_{i,k}\})$ (denoted as 'resolution' in the legend). The upper row refers to the enriched PPUM using a preconditioner based on the L^2-norm, i.e., the local mass matrix, the lower row refers to the enriched PPUM using a preconditioner based on the H^1-norm, i.e., the local stiffness matrix. In both cases we used a cut-off parameter of $\epsilon = 10^{-12}$.

off for the L^2-based projection and almost no reduction in degrees of freedom for the H^1-based projection. Hence, the nonnestedness of the respective local approximation spaces is as expected more severe for the L^2-based projection than for the H^1-based projection.

In summary, the presented hierarchical enrichment scheme yields a globally optimal convergence behavior of $O(h)$ in the energy-norm for the uniform h-version of the enriched PPUM without compromising the condition number of the resulting stiffness matrix. This is achieved by a local preconditioner which eliminates the near-null space of an arbitrary local operator. Within the enrichment zone the hierarchically enriched PPUM yields a convergence rate of $O(h^{1+\delta})$ in the energy-norm with $\delta > 0$.

5 Concluding Remarks

We presented an automatic hierarchical enrichment scheme for the PPUM which yields a stable discretization with optimal convergence properties globally and a kind of superconvergence within the employed enrichment zone. The core ingredients of the presented approach are a geometric hierarchy of the cover patches and a special local preconditioner. The construction of the presented preconditioner relies on the flat-top property of the employed PU.

Table 3. Relative errors e (4.1) and convergence rates ρ (4.2) with respect to the subsets E_1, E_2, and E_3 from (4.9). The local projections $\Pi^*_{i,k}$ are based on the H^1-norm.

J	dof	N	e_{L^∞}	ρ_{L^∞}	e_{L^2}	ρ_{L^2}	e_{H^1}	ρ_{H^1}
with respect to E_1								
2	28	4	4.329_{-2}	0.94	3.245_{-2}	1.03	9.040_{-2}	0.72
3	70	16	3.145_{-2}	0.35	2.061_{-2}	0.50	6.313_{-2}	0.39
4	178	36	1.058_{-2}	1.17	5.325_{-3}	1.45	2.559_{-2}	0.97
5	562	100	3.385_{-3}	0.99	1.390_{-3}	1.17	9.671_{-3}	0.85
6	2002	324	1.018_{-3}	0.95	3.534_{-4}	1.08	3.495_{-3}	0.80
7	7570	1156	2.974_{-4}	0.93	8.867_{-5}	1.04	1.270_{-3}	0.76
8	27516	4356	8.477_{-5}	0.97	2.217_{-5}	1.07	4.613_{-4}	0.78
9	101490	16900	2.387_{-5}	0.97	5.539_{-6}	1.06	1.548_{-4}	0.84
10	397538	66564	6.632_{-6}	0.94	1.384_{-6}	1.02	5.701_{-5}	0.73
with respect to E_2								
3	28	4	1.659_{-2}	1.23	1.178_{-2}	1.33	3.599_{-2}	1.00
4	112	16	4.200_{-3}	0.99	3.707_{-3}	0.83	1.216_{-2}	0.78
5	252	36	1.209_{-3}	1.54	8.846_{-4}	1.77	4.271_{-3}	1.29
6	700	100	3.040_{-4}	1.35	2.133_{-4}	1.39	1.472_{-3}	1.04
7	2268	324	7.327_{-5}	1.21	5.209_{-5}	1.20	5.182_{-4}	0.89
8	8092	1156	1.819_{-5}	1.10	1.287_{-5}	1.10	1.849_{-4}	0.81
9	27768	4356	4.556_{-6}	1.12	3.200_{-6}	1.13	6.193_{-5}	0.89
10	102632	16900	1.142_{-6}	1.06	7.982_{-7}	1.06	2.702_{-5}	0.63
with respect to E_3								
4	28	4	3.567_{-3}	1.69	2.447_{-3}	1.80	1.096_{-2}	1.35
5	112	16	9.241_{-4}	0.97	7.710_{-4}	0.83	4.124_{-3}	0.70
6	252	36	2.651_{-4}	1.54	1.803_{-4}	1.79	1.471_{-3}	1.27
7	700	100	6.244_{-5}	1.42	4.337_{-5}	1.39	5.247_{-4}	1.01
8	2268	324	1.495_{-5}	1.22	1.056_{-5}	1.20	1.882_{-4}	0.87
9	8092	1156	3.685_{-6}	1.10	2.606_{-6}	1.10	6.133_{-5}	0.88
10	27368	4356	9.081_{-7}	1.15	6.484_{-7}	1.14	3.038_{-5}	0.58

Acknowledgement. This work was supported in part by the Sonderforschungsbereich 611 *Singular phenomena and scaling in mathematical models* funded by the *Deutsche Forschungsgemeinschaft.*

References

1. I. Babuška, U. Banerjee, and J. E. Osborn, *Survey of Meshless and Generalized Finite Element Methods: A Unified Approach*, Acta Numerica, (2003), pp. 1–125.
2. I. Babuška and J. M. Melenk, *The Partition of Unity Method*, Int. J. Numer. Meth. Engrg., 40 (1997), pp. 727–758.
3. S. Beissel and T. Belytschko, *Nodal Integration of the Element-Free Galerkin Method*, Comput. Meth. Appl. Mech. Engrg., 139 (1996), pp. 49–74.
4. T. Belytschko and T. Black, *Elastic crack growth in finite elements with minimal remeshing*, Int. J. Numer. Meth. Engrg., 45 (1999), pp. 601–620.
5. T. Belytschko, Y. Y. Lu, and L. Gu, *Crack propagation by element-free galerkin methods*, Engrg. Frac. Mech., 51 (1995), pp. 295–315.
6. T. Belytschko, N. Moës, S. Usui, and C. Parimi, *Arbitrary discontinuities in finite elements*, Int. J. Numer. Meth. Engrg., 50 (2001), pp. 993–1013.
7. E. Chahine, P. Laborde, J. Pommier, Y. Renard, and M. Salaün, *Study of some optimal xfem type methods*, in Advances in Meshfree Techniques, V. M. A.

Leitao, C. J. S. Alves, and C. A. M. Duarte, eds., vol. 5 of Computational Methods in Applied Sciences, Springer, 2007.
8. J. S. Chen, C. T. Wu, S. Yoon, and Y. You, *A Stabilized Conforming Nodal Integration for Galerkin Mesh-free Methods*, Int. J. Numer. Meth. Engrg., 50 (2001), pp. 435–466.
9. J. Dolbow and T. Belytschko, *Numerical Integration of the Galerkin Weak Form in Meshfree Methods*, Comput. Mech., 23 (1999), pp. 219–230.
10. C. A. Duarte, L. G. Reno, and A. Simone, *A higher order generalized fem for through-the-thickness branched cracks*, Int. J. Numer. Meth. Engrg., 72 (2007), pp. 325–351.
11. C. A. M. Duarte, I. Babuška, and J. T. Oden, *Generalized Finite Element Methods for Three Dimensional Structural Mechanics Problems*, Comput. Struc., 77 (2000), pp. 215–232.
12. C. A. M. Duarte, O. N. H. T. J. Liszka, and W. W. Tworzydlo, *A generalized finite element method for the simulation of three-dimensional dynamic crack propagation*, Int. J. Numer. Meth. Engrg., 190 (2001), pp. 2227–2262.
13. M. Griebel, P. Oswald, and M. A. Schweitzer, *A Particle-Partition of Unity Method—Part VI: A p-robust Multilevel Preconditioner*, in Meshfree Methods for Partial Differential Equations II, M. Griebel and M. A. Schweitzer, eds., vol. 43 of Lecture Notes in Computational Science and Engineering, Springer, 2005, pp. 71–92.
14. M. Griebel and M. A. Schweitzer, *A Particle-Partition of Unity Method—Part II: Efficient Cover Construction and Reliable Integration*, SIAM J. Sci. Comput., 23 (2002), pp. 1655–1682.
15. ———, *A Particle-Partition of Unity Method—Part III: A Multilevel Solver*, SIAM J. Sci. Comput., 24 (2002), pp. 377–409.
16. ———, *A Particle-Partition of Unity Method—Part V: Boundary Conditions*, in Geometric Analysis and Nonlinear Partial Differential Equations, S. Hildebrandt and H. Karcher, eds., Springer, 2002, pp. 517–540.
17. ———, *A Particle-Partition of Unity Method—Part VII: Adaptivity*, in Meshfree Methods for Partial Differential Equations III, M. Griebel and M. A. Schweitzer, eds., vol. 57 of Lecture Notes in Computational Science and Engineering, Springer, 2006, pp. 121–148.
18. N. Moës, J. Dolbow, and T. Belytschko, *A finite element method for crack growth without remeshing*, Int. J. Numer. Meth. Engrg., 46 (1999), pp. 131–150.
19. J. Nitsche, *Über ein Variationsprinzip zur Lösung von Dirichlet-Problemen bei Verwendung von Teilräumen, die keinen Randbedingungen unterworfen sind*, Abh. Math. Sem. Univ. Hamburg, 36 (1970–1971), pp. 9–15.
20. J. T. Oden and C. A. Duarte, *Clouds, Cracks and FEM's*, Recent Developments in Computational and Applied Mechanics, 1997, pp. 302–321.
21. M. A. Schweitzer, *A Parallel Multilevel Partition of Unity Method for Elliptic Partial Differential Equations*, vol. 29 of Lecture Notes in Computational Science and Engineering, Springer, 2003.
22. ———, *An adaptive hp-version of the multilevel particle–partition of unity method*, Comput. Meth. Appl. Mech. Engrg., (2008). accepted.

Bestellungen nimmt entgegen:

Institut für Angewandte Mathematik
der Universität Bonn
Sonderforschungsbereich 611
Wegelerstr. 6
D - 53115 Bonn

Telefon: 0228/73 4882
Telefax: 0228/73 7864
E-mail: astrid.link@iam.uni-bonn.de http://www.sfb611.iam.uni-bonn.de/

Verzeichnis der erschienenen Preprints ab No. 355

355. Löbach, Dominique: On Regularity for Plasticity with Hardening

356. Burstedde, Carsten; Kunoth, Angela: A Wavelet-Based Nested Iteration – Inexact Conjugate Gradient Algorithm for Adaptively Solving Elliptic PDEs

357. Alt, Hans-Wilhelm; Alt, Wolfgang: Phase Boundary Dynamics: Transitions between Ordered and Disordered Lipid Monolayers

358. Müller, Werner: Weyl's Law in the Theory of Automorphic Forms

359. Frehse, Jens; Löbach, Dominique: Hölder Continuity for the Displacements in Isotropic and Kinematic Hardening with von Mises Yield Criterion

360. Kassmann, Moritz: The Classical Harnack Inequality Fails for Non-Local Operators

361. Albeverio, Sergio; Ayupov, Shavkat A.; Kudaybergenov, Karim K.: Description of Derivations on Measurable Operator Algebras of Type I

362. Albeverio, Sergio; Ayupov, Shavkat A.; Zaitov, Adilbek A.; Ruziev, Jalol E.: Algebras of Unbounded Operators over the Ring of Measurable Functions and their Derivations and Automorphisms

363. Albeverio, Sergio; Ayupov, Shavkat A.; Zaitov, Adilbek A.: On Metrizability of the Space of Order-Preserving Functionals

364. Alberti, Giovanni; Choksi, Rustum; Otto, Felix: Uniform Energy Distribution for Minimizers of an Isoperimetric Problem Containing Long-Range Interactions

365. Schweitzer, Marc Alexander: An Adaptive hp-Version of the Multilevel Particle-Partition of Unity Method

366. Frehse, Jens; Meinel, Joanna: An Irregular Complex Valued Solution to a Scalar Linear Parabolic Equation

367. Bonaccorsi, Stefano; Marinelli, Carlo; Ziglio, Giacomo: Stochastic FitzHugh-Nagumo Equations on Networks with Impulsive Noise

368. Griebel, Michael; Metsch, Bram; Schweitzer, Marc Alexander: Coarse Grid Classification: AMG on Parallel Computers

369. Bar, Leah; Berkels, Benjamin; Rumpf, Martin; Sapiro, Guillermo: A Variational Framework for Simultaneous Motion Estimation and Restoration of Motion-Blurred Video; erscheint in: International Conference on Computer Vision 2007

370. Han, Jingfeng; Berkels, Benjamin; Droske, Marc; Hornegger, Joachim; Rumpf, Martin; Schaller, Carlo; Scorzin, Jasmin; Urbach Horst: Mumford–Shah Model for One-to-one Edge Matching; erscheint in: IEEE Transactions on Image Processing

371. Conti, Sergio; Held, Harald; Pach, Martin; Rumpf, Martin; Schultz, Rüdiger: Shape Optimization under Uncertainty – a Stochastic Programming Perspective

372. Liehr, Florian; Preusser, Tobias; Rumpf, Martin; Sauter, Stefan; Schwen, Lars Ole: Composite Finite Elements for 3D Image Based Computing

373. Bonciocat, Anca-Iuliana; Sturm, Karl-Theodor: Mass Transportation and Rough Curvature Bounds for Discrete Spaces

374. Steiner, Jutta: Compactness for the Asymmetric Bloch Wall

375. Bensoussan, Alain; Frehse, Jens: On Diagonal Elliptic and Parabolic Systems with Super-Quadratic Hamiltonians

376. Frehse, Jens; Specovius-Neugebauer, Maria: Morrey Estimates and Hölder Continuity for Solutions to Parabolic Equations with Entropy Inequalities

377. Albeverio, Sergio; Ayupov, Shavkat A.; Omirov, Bakhrom A.; Turdibaev, Rustam M.: Cartan Subalgebras of Leibniz n-Algebras

378. Schweitzer, Marc Alexander: A Particle-Partition of Unity Method – Part VIII: Hierarchical Enrichment